

Modelo puntal tensor para un nudo híbrido viga de hormigón y viga de acero bajo cargas gravitatorias

Strut and tie model for a hybrid nodes in beam of concrete and steel beam under gravitatory loads

Y. Mieles^{1*}, R. Larrúa^{**}

* Universidad Técnica de Manabí – Portoviejo, ECUADOR

** Universidad de Camagüey – Camagüey, CUBA

Fecha de Recepción: 11/04/2019

Fecha de Aceptación: 22/07/2019

PAG 330-343

Abstract

Experimental tests carried out in the laboratory of structures of the National Polytechnic School (Ecuador) in beams with hybrid nodes, increasingly used in the construction of buildings with steel deck slabs, demonstrated that the hybrid nodes does not decrease the strength of concrete beams, reaching approximate values to the theoretical ones for the beam without nodes.

With the results of the experimentation and models in finite elements, the trajectory of efforts to perform a Strut and Tie Model (STM) was sought, obtaining areas of steel 15% superior to the design with the flexion formulas of the ACI 318-14. General formulas of the STM are presented for beams of any light with a single hybrid nodes, but it is possible to extend them to several nodes. The experimental evidence and STM shows that the point load is transferred better with the steel beam penetrating the concrete beam, which does not decrease the strength.

Keywords: Hybrid nodes, steel deck, strut and tie, concrete beams, experimental tests

Resumen

Ensayos experimentales realizados en el laboratorio de estructuras de la Escuela Politécnica Nacional (Ecuador) en vigas con nudos híbridos, cada vez más utilizados en la construcción de edificios con losas steel deck, demostraron que el nudo híbrido no disminuye la resistencia de las vigas de hormigón, alcanzando valores aproximados a los teóricos para la viga sin nudo.

Con los resultados de la experimentación y modelos en elementos finitos se buscó la trayectoria de esfuerzos para realizar un Modelo Puntal Tensor (MPT), obteniendo áreas de acero 15% superior al diseño con las fórmulas de flexión del ACI 318-14. Se presentan formulas generales del MPT para vigas de cualquier luz con un solo nudo híbrido, pero es posible extenderlas a varios nudos. La evidencia experimental y MPT muestra que la carga puntual se transfiere mejor con la viga de acero penetrando a la viga de hormigón, la cual no disminuye la resistencia.

Palabras clave: Nudo híbrido; steel deck; puntal tensor; vigas de hormigón; ensayos experimentales

1. Introduction

The hybrid nodes are the result of seeking a constructive solution to steel deck mezzanines on metal beams connected to reinforced concrete beams. The steel deck is supported by steel beams and connected to reinforced concrete beams by constructive alternatives and dispersions described in (Mieles and Castañeda, 2016a), Mieles and Castañeda, 2016b), such as those shown in Figure 1.a, where the steel beam crosses or Figure 1.b where it is mechanically anchored to the reinforced concrete beam. Figures 1.c and 1.d illustrate how the steel beams support the steel deck.

The incorrect design of hybrid nodes in beams caused structural damage in the earthquake in Ecuador on April 16, 2018, of 7.8 (Mw), referred to in (Castañeda and Mieles, 2016) (Castañeda and Mieles, 2017). A node is defined as the joint of two or more structural elements that converge at a point that moves and rotates, where the fields of compression or traction of the ties intersect (EHE-08, 2008) (NSR, 2012), its design is considered to be critical due to failures attributed to the lack of detail of the node (Aguiar et al., 2010); in seismic zones, it receives a lot of importance. For this reason, the code ACI 318-14 specifies the philosophy of a strong node-weak beam (Aguiar, 2014). The connection must meet the requirements of chapter 18 of ACI 318-14 and ACI 352, it must resist the stresses of the structural elements and transmit concurring forces such as axial, bending, torsion and shear (Nilson et al., 2010) (ACI-318S-14, 2014).

The disturbed zone of the hybrid node does not comply with the linear distribution of deformations, the Bernoulli's principle of flatness of a B region is a geometric discontinuity known as the D region. Discontinuity due to change of geometry, connections, hybrid nodes, the passage of pipes through the beam web, load or concentrated reaction, are regions with a turbulent stress path (ACI-318S-14, 2014). The design of a hybrid node with the classic

¹ Corresponding author:

Universidad Técnica de Manabí – Portoviejo, ECUADOR

E-mail: yordimieles@gmail.com

theory of bending and shear for beams in the *D* region is not recommended. Currently, empiricism, reinforcement detailing, or designer experience are used. However, this does not guarantee an appropriate design. The ACI 318-14 does not specifically address a hybrid node, but the Strut and Tie

Model (STM) is an alternative for designing discontinuity regions (Reineck, 2002). The STM can be applied once the distribution of stresses in the *D* region is known, supported by experimental models (Schlaich et al., 1987).



Figure 1. Hybrid Nodes a) drop-in profile I, b) anchored profile I, c and d) steel deck slab

The Saint-Venant's Principle states that the disturbance extends for a length equal to the largest cross-section dimension, measured from the point where it occurs, the limit from which the stresses approach a linear distribution (ACI-318S-14, 2014; Schlaich et al., 1987). The STM idealizes as a truss the *D* region from the direction of the normal and tangential stresses in the disturbed section, defining the trajectory and location of the struts and ties to transfer the stresses to the *B* region. The geometry of the struts and ties is performed with finite element elastic analysis, which establishes the extent and direction of the main compressive and tensile stresses (Wight and MacGregor, 2012) which must be verified through real experiments with hybrid node beams.

The literature reviewed for mixed nodes or joints includes: the ACI 318-14 in 16.4 recommends for a connection composed of a member subject to bending the complete transfer of shear force on the surfaces by stirrups, the shear strength at the contact of the surfaces or both. The (ASCE, 1994) in "Task Committee on Design Criteria for

Composite Structures in Steel and Concrete" gives details and recommendations for mixed continuous steel beam connections through the concrete column as shown in (Figure 2.a).

Other contributions on mixed concrete-steel joints are: (Kuramoto and Nishiyama, 2004) presented research on the so-called "through-column-type beam-to-column joint" node (Figure 2.b). (Nie et al., 2008) present a mixed node of steel tubular column to concrete beam, (Chen et al., 2015) the "through-beam connection" system (Figure 2.c). (Aznar et al., 2008) present a study and experiments of metal column coupled to a concrete beam (Figure 2.d). (Li et al., 2011) propose hybrid nodes of reinforced concrete and steel, called "steel-SRC hybrid structure system", (Soto, 2012) studies the connection of steel beams to concrete walls. (Ugel, 2015) proposes a method for assessing seismic vulnerability and damage in mixed steel-reinforced concrete structures, as well as a methodology for the design of shear and moment resistant mixed rigid joints.

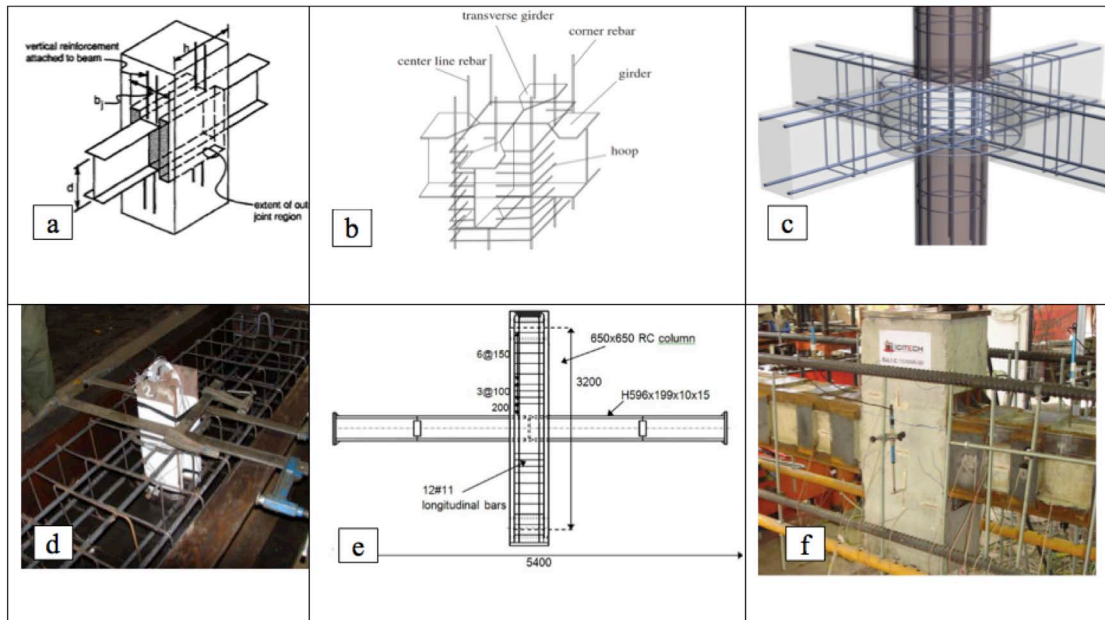


Figure 2. Different mixed or hybrid nodes studied by various authors, (ASCE, 1994), (Kuramoto and Nishiyama, 2004), (Chen et al., 2015), (Aznar et al., 2008), (Rasoul and Bakhshayesh, 2013), (Garzón, 2013)

(Rasoul and Bakhshayesh, 2013) present a hybrid node between a steel beam passing through a concrete column (Figure 2.e) later validated with an experimental test that concludes that the hybrid node is better than the traditional nodes (Rasoul, Bakhshayesh, & Mehdi, 2016). (Garzón, 2013) studies a concrete node that is reinforced with steel plates as shown in Figure 2.f. A post-tensioned hybrid connection in prefabricated columns studied by (Marcus and Thiers, 2015) is also used as a means of dissipating energy at the joint and maintaining the initial stiffness of the structure.

For this work, 12 experimental models of beams with hybrid nodes were made and tested in the Housing Laboratory of the National Polytechnic School (from the Spanish Laboratorio de la Vivienda de la Escuela Politécnica Nacional), Ecuador. The objective of the experimental tests of

beams with hybrid nodes is to verify the structural behavior, to answer to the uncertainty of this type of nodes, the mechanism and progress of the failure and to calibrate computer models of finite elements, STM and finally to look for the way to improve the connection.

2. Characteristics of the experimental tests

The models represent the two most observed types of nodes in the construction of hybrid node beams. The beams tested had a width of $b = 25$ cm which is the minimum standard of the American Concrete Institute (ACI-318S-14, 2014), a height of $h = 40$ cm, approximately 1.5 times the width of the beam (Figure 3).

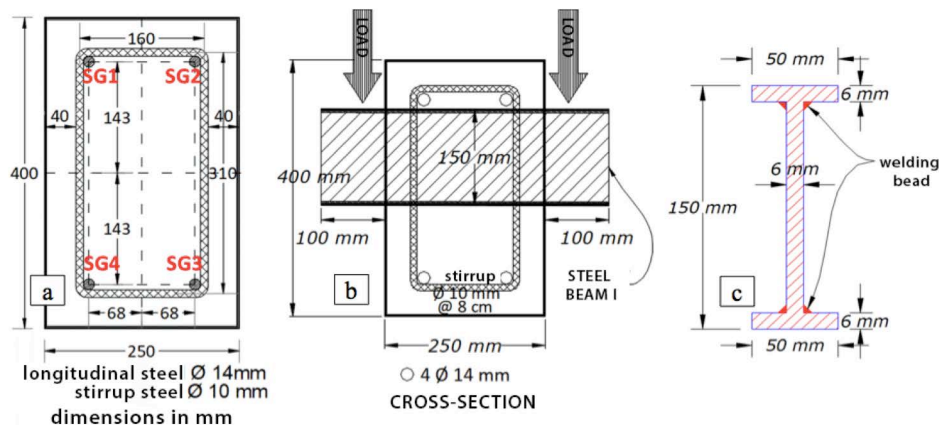


Figure 3. Beam geometry. a) cross-section. b) location of the node, c) cross-section of the steel beam

The longitudinal steel area is slightly greater than the minimum steel $2\phi 14\text{mm}$, the average compressive strength of the concrete is 21 MPa, standard stirrups are 10 mm and 8 cm of separation, they provide a nominal moment (without the reduction factor of $\phi = 0.90$ y 0.85 for f'_c) in the cross-section of 42.78 kN-m, the point load for the specimen span (see Figure 6) is 100.65 kN. The acronym SG in Figure 3.a

marks the location of four strain gauges on the steel bars around the node. The location of the node and the steel beam are shown in (Figure 3.b) and (Figure 3.c), for two types of nodes tested: the through node and a node connected by means of anchorage hooks shown in Figure 4, which reproduces the pictures of (Figure 1.a) and (Figure 1.b).

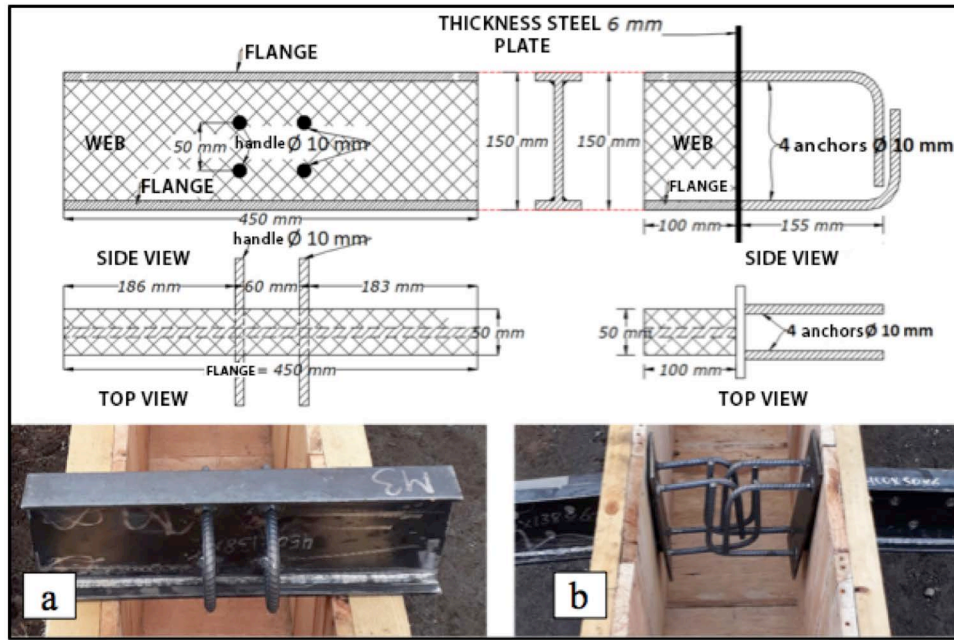


Figure 4. Types of nodes a) through node b) anchored node

The load was applied in the lateral direction of the beam (Figure 5.a) and vertically (Figure 5.b).

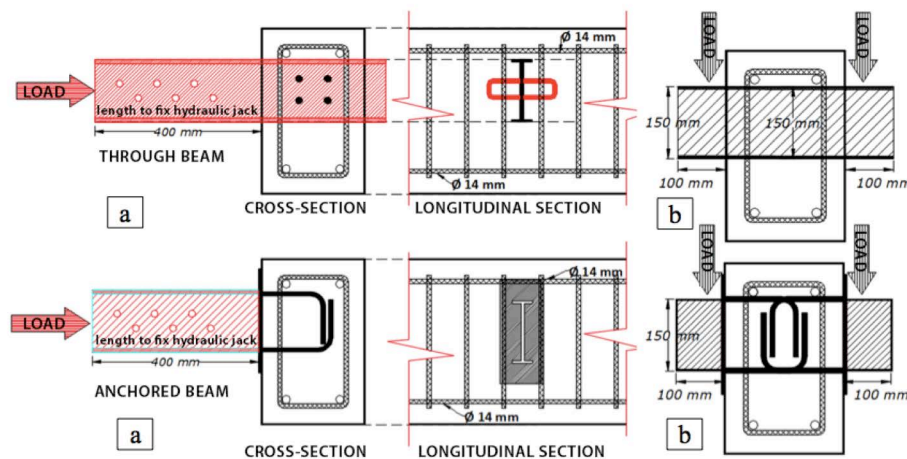


Figure 5. Load application a) lateral direction b) vertical direction

2.1 Vertical load tests

The MA and MC models tested with vertical load parallel to axis 2-2 of the beam to generate bending stresses around axis 3 and shear stresses in axis 2, (axes shown in (Figure 6.d)). There were three specimens for each case. The objective was to observe the bending and shearing performance of the beam, the failure mechanism and the way

the load is transmitted. The load was applied to the steel beam in the direction of gravity, as they work in service, and shown in Figure 6, to represent the way the steel deck slabs transmit most of the weight to the concrete beam. Displacements were measured with three Linear Variable Differential Transformers, (LVDTs) outlined in (Figure 6.c), and monotonic loads until the element was led to failure.

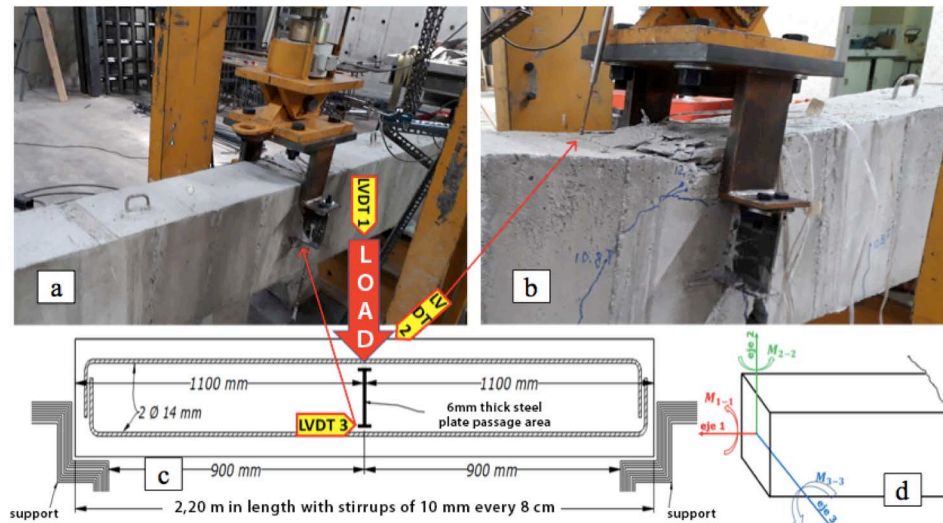


Figure 6. Application of the load in the vertical direction on MC and MD models

(Figure 7) shows that the slope of the load-deformation curve is the same for tensile and compressed steels until the concrete reaches its maximum strength, which occurs in the order of deformations of $\epsilon = 0.0001$ (Mander et al., 1988). From that point on, the load curve starts to slope

differently from the deformation curve. (Figure 7c) and (Figure 7d) are Abaqus models and illustrate the deformations and stresses in the 1-1 directions of the beam, showing the formation of compression struts in the area under the mixed connection.

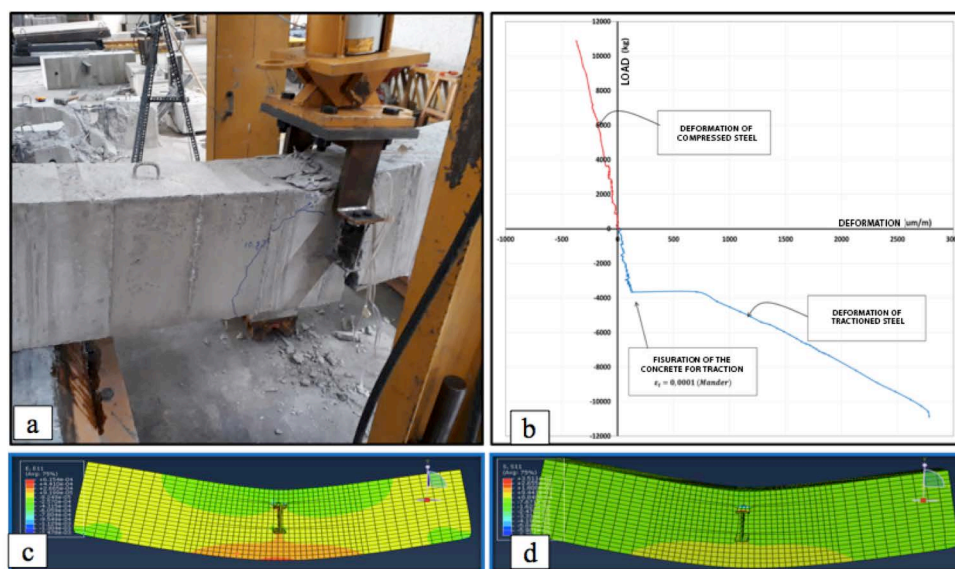


Figure 7. Model MC2, a) tested model; b) Deformation of tensile and compressed steel; c) Deformation in direction 1-1; d) Stresses in direction 1-1

(Figure 8) shows the load-deformation behavior of the 4 strain gauges and the load-displacement curve of 3 LVDT sensors placed in the node section. The THEORETICAL MODEL column in (Table 1) shows the theoretical failure load of 100.65 kN without reduction coefficients $\phi = 0.9$ y 0.85 de f'_c calculated with the ACI formulas for bending beams, recognizing at this point that the node is D region and

it is not appropriate to apply those formulas. This value is lower than the average load obtained from the experiment that originates the yielding in the 103 kN tensile steel, under the FAILURE LOAD column in (Table 1) and represented in (Figure 8). Before the theoretical failure, obvious cracking begins, with the first cracks visible for a load of approximately 78 kN in all models.

Table 1. Loading values and yield moment of the tensile steel.

VERTICAL LOAD				
EXPERIMENTAL MODELS			THEORETICAL MODEL, ACI BENDING FORMULAS (without strength reduction factors)	
MODEL	FAILURE LOAD	FAILURE MOMENT	FAILURE LOAD	FAILURE MOMENT
	kN	kN-m	kN	kN-m
MC1	106.93	48.12	100.65	42.78
MC2	103.99	46.79		
MC3	115.76	52.09		
MD1	100.36	45.16		
MD2	95.16	42.82		
MD3	97.12	43.70		
PROMEDIO≈	103.22	46.45		

(Figure 8) shows that compressed steel has a higher elastic behavior, tensile steel a first elastic stage until the concrete deforms $\epsilon_c = 0,0001$ at a load of 35.86 kN (3656 kg), then the steel goes into yielding at typical deformations

greater than 0.002 and the beam fails at a load greater than the theoretical load. It was concluded that the node does not decrease the bending strength of the beam.

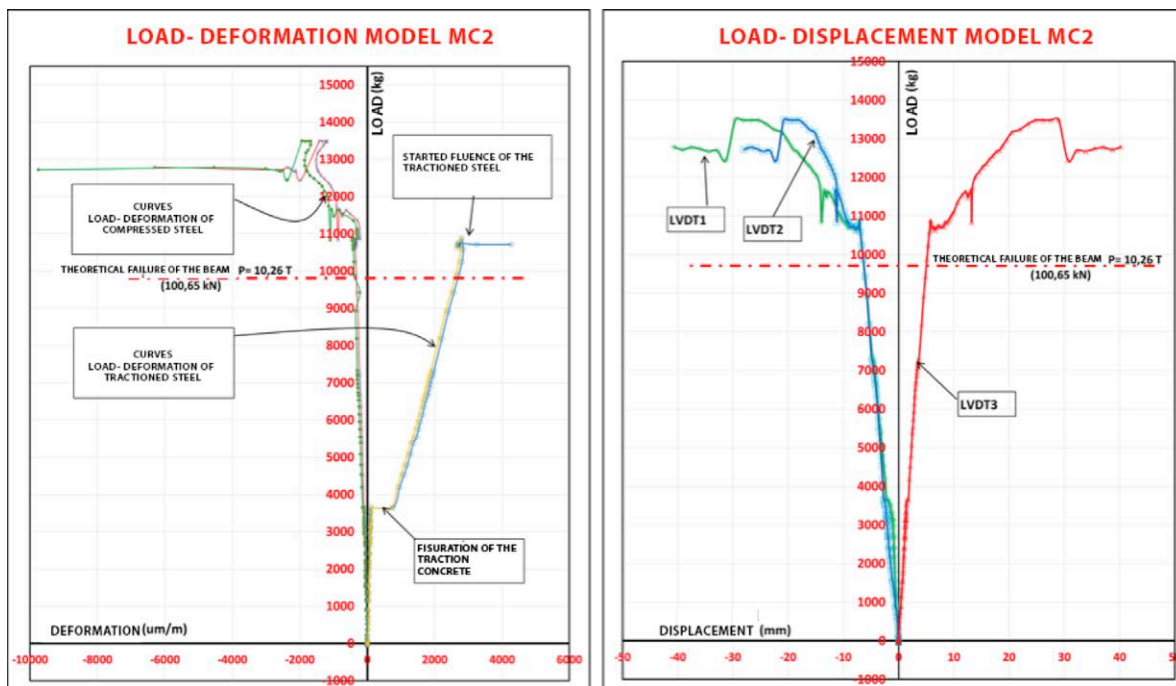


Figure 8. Model MC2 curve; a) load-deformation curve; b) load-displacement curve



2.2 Horizontal load tests

Three specimens were tested with a horizontal load named MA in order to observe the penetration hardness of the steel beam through the node. The load is applied in the longitudinal direction to the steel beam 1, parallel to the axis 3

of the beam. See the diagram in (Figure 9). It was equipped with two LVDT sensors and 4 strain gauges as shown in Figure 3.a. The steel beam had two handle-shaped steels to prevent slippage.

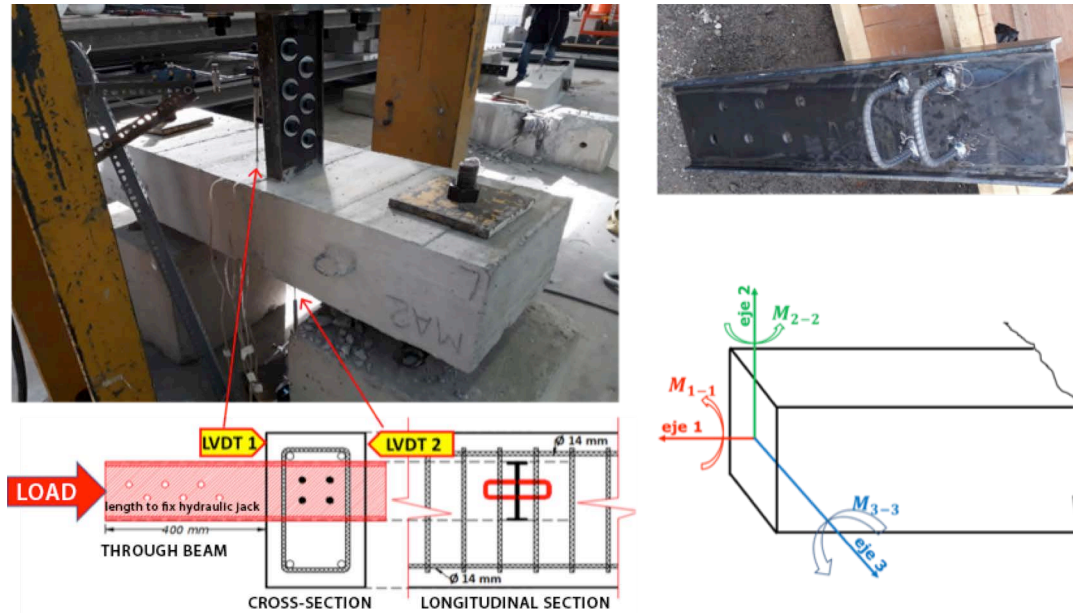


Figure 9. MA models tested in the longitudinal direction of the node



Figure 10. MA models tested in the longitudinal direction of the node

The evolution of the damage observed in the experiments, such as the damage shown in Figure 10 and the graphs in (Figure 11), demonstrate that the collapse is due to the shear failure of the steel beam and that the longitudinal tensile or compressive reinforcement of the concrete beam does not reach yielding.

In (Castañeda and Miele, 2017) computer models of buildings with hybrid nodes with three independent variables and two levels were made (experiment 2^3): height of the building, rectangularity in floor plan and type of node; in all cases, it was found that the type of node influences the structural response of the dependent variables moment, shear

and floor drift. In these same computer models, the maximum axial force of the hybrid node steel beams was sought. The results, which were less than 1 kN, compared with the axial force results of the experimental test in the structure laboratory, indicate that a good behavior of the node without anchors can be expected under axial load, also the continuity of the secondary steel beam must be added. The laboratory test record shown in (Figure 11) for load-deformation indicates that the first tensile yield of the concrete is stronger than the maximum possible stress of the models of computer experiment 2^3 for the horizontal load.

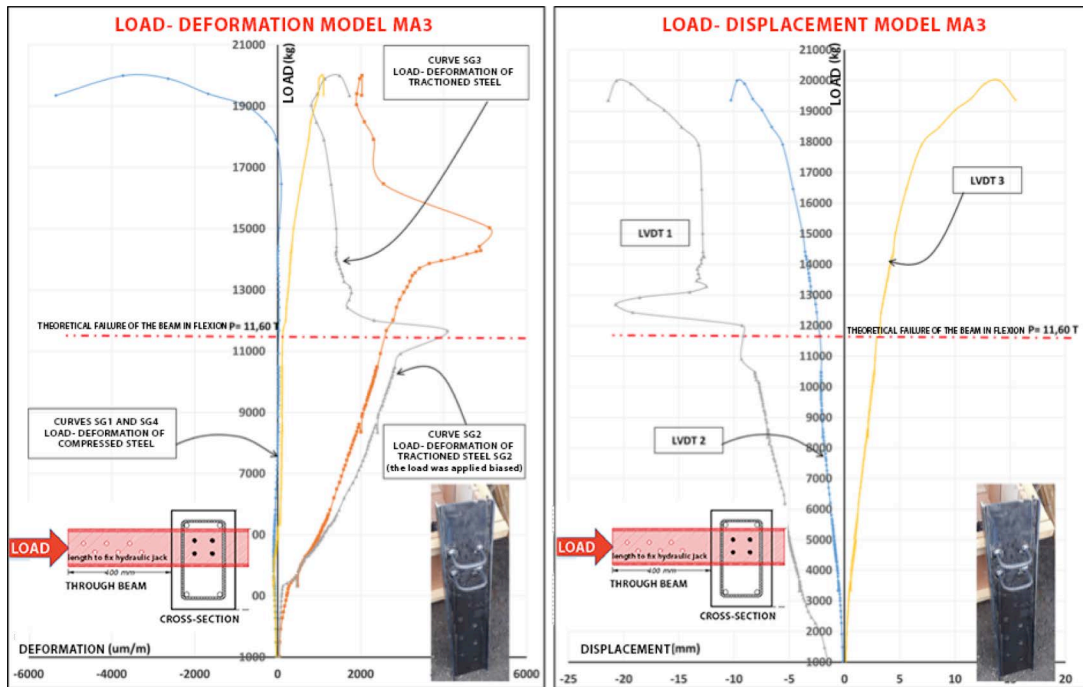


Figure 11. MA models tested in the longitudinal direction of the node

This is due to the fact that the design of the concrete beam and the node are dominated by moments acting around axis 3 see (Figure 9). The moments of axis 2 do not dominate the design, as the lateral load is mostly taken up by the concrete nodes and frames. The hybrid node takes little axial load since the steel beam has little stiffness compared to parallel concrete beams. If the accepted deformation for

simple tensile concrete is compared with the deformations of the strain gauges placed on the horizontal experimental test beams in (Figure 11), it can be seen that the service axial forces of a building with hybrid nodes do not govern the behavior of the node. However, it is advisable to use some kind of anchorage in the hybrid node according to the axial load as shown in (Figure 12).



Figura 12. Opciones de unir una viga secundaria a una de principal o columna

2.3 Comparison with previous node failure experiences

On April 16, 2016, a 7.8 (Mw) earthquake occurred in Ecuador which had its epicenter in the coastal province of Manabí. Many buildings collapsed and others were damaged. The authors of this study inspected the behavior of buildings with hybrid nodes and steel deck slabs after the earthquake. The damages described were presented in (Castañeda and Miele, 2017) (Castañeda and Miele, 2016). Comparing the damages of the natural laboratory of the earthquake with the tested nodes it is observed that the cracking form coincides, as it is observed in the pictures of this article and pictures of the aforementioned works.

3. Strut and Tie Model for a hybrid node

The analysis and design of structures are made to sections and stresses are verified such as moment and cut, contrary to the essence of the codes that deal with entire structures and overall security (Aguar, 2014). The risk of this sectional approach is the possibility of ignoring the general flow of forces and not covering critical D regions that are built with code detailing rules to ensure overall security. The strut and tie model unifies the design concept of the B and D

regions with similar models when sectional design procedures for bending and shearing cannot be applied (Reineck, 2002).

An applied point load (such as that transmitted by the steel beam to the concrete beam) induces a D region in a length close to the height "d" of the beam. ACI 318-14 also clarifies in point 9.9.1.1 that if the load is applied to the side or bottom, the STM is used because it does not meet linear deformation (ACI-318S-14, 2014). There are several methods for determining the geometry of the strut and tie model such as the stress path through elastic analysis, finite elements, loading paths (Schlaich et al., 1987). A two-dimensional model is then used to represent flat structures such as high-rise beams, cantilevers, and connections, where the cracking pattern in similar structures helps "locating the struts and ties within the structure so that the ties are located between the cracks" (MacGregor, 2002).

The node tends to resist with the least amount of deformation work among all possible STM models. For small loads that do not exceed the cracking value of the tensile concrete and small deformations of steel, a strut is first formed under the point load until the micro-cracks in the concrete accommodate forces and the steel starts to take over the tensions. The STM is checked with the tested beams. Figure 13 shows the typical form of damage, 13.b is a bottom view of the beam and 13.d shows the strut that is formed by the thrust of the steel beam.



Figure 13. Form of damage in the tested beam

3.1 Strut and Tie Model

The geometry of the struts and ties has been located by the observation of the damage progress during the test

(Figure 14.a) and (Figure 15.b), it is verified by the deformations and stresses in the direction 1-1 of the models in finite elements in Abaqus of (Figure 7.c) and (Figure 7.d.)

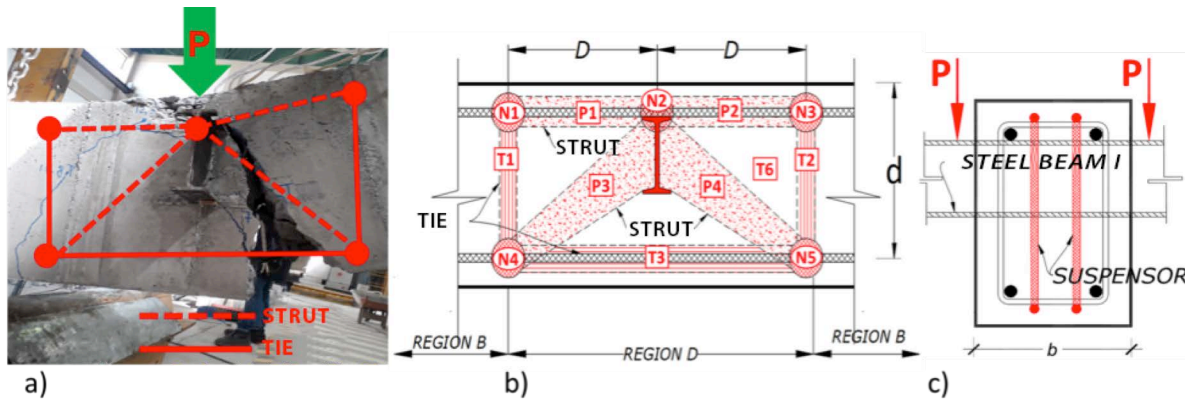


Figure 14. Strut and tie model, a) Damage observed in the test, b) Geometry of struts, c) Suspension proposal.

In the STM in (Figure 14) and (Figure 15), the strut angles P_3 and P_4 are greater than 25 degrees and comply with 23.2.7 of ACI 318-14. The length of D region, (Figure 14.b), according to the Saint Venant principle will have the same length as twice the effective height "d", resulting in the geometry and balance of struts and ties shown in Figure 15, then, transmitting these stresses to region B.

The forces F_{us} or F_{ut} on the STM reinforcement for any hybrid node beam can be generalized by naming the span on each side of the node as $l_1 = n_1 d$ and $l_2 = n_2 d$, respectively (see Figure 15) and the total span as $l = n d$. Once the reinforcement is solved, the forces on the struts and ties in the node area are summarized in (Table 2) and (Table 3).

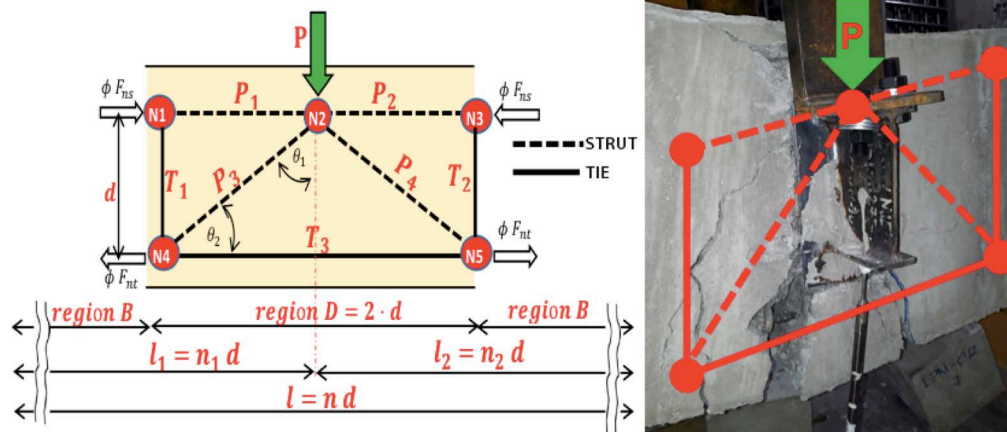


Figure 15. Identification of struts and ties for the STM of the hybrid node

The width of the b_f flange of the steel beam serves as a support plate against the action of P load and when passing through the hybrid node it needs to develop a concrete strength in the node zone 2 greater than or equal to the compressive force of P load and to comply with $F_{nn} \geq F_{us}$, where F_{nn} is the strength in the face of the hydrostatic node zone 2, also guaranteeing the strength of that node zone CCC

since all the concurrent forces are less than or equal to P. It can be shown that $F_{us} = P$, then $P \leq \phi F_{nn} \cdot \text{area of beam I}$, where $\phi=0,75$ and $\beta_n = 1$. The width of the flange that acts as a support plate for the steel beam must be greater than or equal to b_f obtained from (Equation 1), where b is the width of the concrete beam:



ENGLISH VERSION.....

$$b_f = \frac{P}{b \phi F_{nn}} \quad (1)$$

To exemplify (Equation 1), it is replaced with the average P of 103 kN obtained in the experiments (Table 1) and the data of the hybrid direction through node explained in Figure 4.3 is obtained that the minimum width is 3.1 cm < 5 cm, satisfies the real width of the drop-in girder 1 and conditions the width of the converging P_3 and P_4 struts.

$$A_{st} = \frac{F_{ut}}{\phi f_y} \quad (2)$$

In the ties, the following must be complied with: $\phi F_{nt} \geq F_{ut}$, where $\phi=0,75$, F_{nt} is the nominal strength of the tie, and F_{ut} , is the factored tractive effort of the tie a relationship that gives rise to (Equation 2). The tensile steel area of the T_i tie is obtained with (Equation 2), making F_{ut}

equals to $T_3 = P \cdot n_2^2/n$ from (Table 2) to generalize to any beam. In order to compare with the A_s of tensile strength resulting from the ACI 318 bending formulas, the factored bending load is used and the moment is calculated with $M_u = \phi A_s f_y (d - a/2)$, and data from (Figure 3). The axial failure load is $P = 4 M_u / l = 90$ kN. The 90 kN in (Equation 2) results in $A_{st3} = 3,57 \text{ cm}^2$, 16% higher than 3.08 cm^2 calculated according to the bending theory. The axis of the T_3 tie is conditioned by the continuity of the steel in the B region and its width w_t can be taken as the diameter of the bars plus twice the cover measured with respect to the surface of the bars according to R23.8 of ACI 318-14.

The steel required for ties T_1 and T_2 can be calculated with (Equation 2), replacing F_{ut} for T_1 and T_2 from (Table 2). The steel thus obtained must be distributed in the form of stirrups in the D region. The summary of the ties is shown in (Table 2) calculated for the average experimental failure load from (Table 1).

Tabla 2. Resumen de fuerzas y áreas de acero de los tensores con carga promedio de ensayo

Tie	F_{ut}		A_{st} (cm^2)	Tie width cm
	Strength of the STM ties of the hybrid node (kN)			
T_1	$T_1 = \frac{P n_2}{n}$	51.50	1.63	9.40
T_2	$T_2 = \frac{P n_1}{n}$	51.50	1.63	9.40
T_3	$T_3 = \frac{P n_2^2}{n}$	128.75	4.09	9.40

Struts must comply with $\phi F_{ns} \geq F_{us}$, where $\phi=0,75$, F_{ns} is the nominal strength of a strut as

defined in 23.4 of ACI 318-14, and F_{us} is the factored compression force of the strut. From these relationships, the width of a strut w_s results from (Equation 3). The strength of the STM struts for the hybrid node, by the action of the P load, is shown in (Table 3), where F_{us} is replaced by the

formulas for P_1 , P_2 and P_r as applicable, $\beta_s = 0,6$ for P_1 y P_2 and $\beta_s = 0,4$ for P_r according to Table 23.4.3 of ACI 318-14.

$$w_s = \frac{F_{us}}{\phi 0,85 \beta_s f'_c b} \quad (3)$$

Tabla 3. Resumen de fuerzas y anchos de los puntales con carga promedio de ensayo

Strut	F_{us} Strength of the STM struts of the hybrid node (kN)		β_s	Strut width (cm)	ϕF_{ns} (kN)
P_1	$P_1 = \frac{P (n_2^2 - n_2)}{n}$	77.25	0.60	3.85	128.750
P_2	$P_2 = \frac{P (n_1^2 - n_1)}{n}$	77.25	0.60	3.85	128.750
P_3	$P_3 = \frac{P n_2}{0,71 n}$	72.54	0.40	5.42	72.535
P_4	$P_4 = \frac{P n_1}{0,71 n}$	72.54	0.40	5.42	72.535

Nodes must comply with $\phi F_{nn} \geq F_{us}$, where $\phi = 0,75$, F_{nn} is the nominal strength of one face of the node, and F_{us} is the factored compressive force of the strut. If the width of the flange of the beam b_f in (Figure 16.a), which serves as the support plate at the node, is greater than or equal to that obtained by (Equation 1), the design strength of the faces of node 2 ϕF_{nn2} will be greater than the forces applied by the struts F_{us} P_1 , P_2 , P_3 y P_4 since the width b_f in (Equation 1) will be greater than the widths required by (Equation 3). In node zone 4, which is symmetrical with 5 in (Figure 16.b), the transfer of stresses to the B region of the tie

T_3 is guaranteed by the continuity of the tensile steel along the beam. The tie T_1 , which must be placed in the form of stirrups, provides the strength by the strut P_3 . For node 1 in (Figure 14.b), the strength of the node zone is ensured by the compression block of the strut P_1 . An application summary of the experimental test carried out with the average failure loads is shown in (Table 4). For node 1 in (Figure 14.b), the strength of the node zone is ensured by the compression block of the prop P_1 . An application summary of the experimental test carried out with the average failure loads is shown in (Table 4).

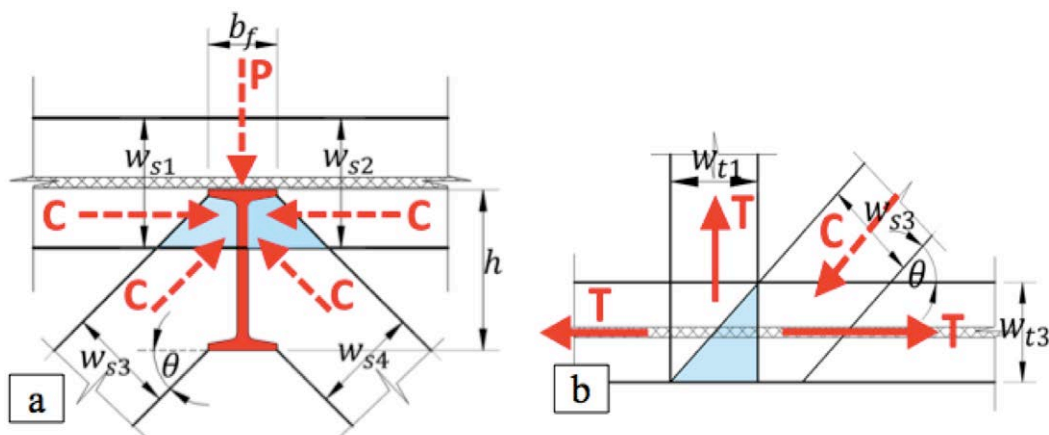


Figure 16. STM nodes. a) Node 2 type CCC according to ACI 318-14; b) Node 4 type CTT according to ACI 318-14

Table 4. STM node verification applied to the tested beams

Node		β_n	f_{ce} (MPa)	Action		F_u (kN)	Width (cm)	F_{nn}	ϕF_{nn}	Compliance	$\frac{\phi F_n}{F_u}$
#	Type			#	Type						
1=3	CCT	0.8	14.28	$P_1=P_2$	C	77.25	3.85	137.33	103.00	SI	1.33
				$T_1=T_2$	T	51.50	9.40	335.58	251.69	SI	4.89
				Cc	C	77.25	3.85	137.33	103.00	SI	1.33
2	CCC	1	17.85	P	C	103.00	5.00	223.13	167.34	SI	1.62
				$P_1=P_2$	C	77.25	3.85	171.67	128.75	SI	1.67
				$P_3=P_4$	C	72.54	5.42	241.78	181.34	SI	2.50
4=5	CTT	0.6	10.71	$P_3=P_4$	C	72.54	5.42	145.07	108.80	SI	1.50
				$T_1=T_2$	T	51.50	9.40	251.69	188.76	SI	3.67
				T_3	T	128.75	9.40	251.69	188.76	SI	1.47

The incorporation of suspensions is proposed for future experimental tests. The total support force must be transferred to the top of the member (beam) using a hanging reinforcement (suspensions) distributed over the width of the web of the support beam, such as those shown in Figure 14.c (FIP, 1999). The transmission of forces from the steel beam to the concrete beam makes it indirect support (ACI-445, 2002). In order to satisfy the balance at the node for the upward forces of the tie rods, suspensions are required. These suspensions or stirrups should be located within the intersection of the web of the main concrete beam and the load-transferring beam (Novak, 2010). An appropriate detail for a node in a beam - concrete beam, requires the use of suspension stirrups well anchored to the main beam (Nilson et al., 2010). Indirect supports have been dealt with in some codes with detailed rules indicating the need to have suspensions, but they have not yet been incorporated in ACI 318-14.

4. Conclusions

The test confirms that even when crossing the steel beam its service life is reliable since the tested beams reach strengths higher than 10% with respect to the theoretical strengths, despite the fact that the strength reduction factors were removed. The initial research assumptions were that the node decreased the strength of the beam but tests have shown that this did not happen. The traditional ACI bending design method that has been used on hybrid node beams already in service is acceptable, although it is admitted that it

is a D region that does not comply with the principles of flatness of the section for the application of the typical bending design formulas of ACI 318-14, but the tests reveal that the strength is approximately equivalent to those formulas, which is attributed to the safety factors of the standards.

The through hybrid node offers greater advantages than the traditional node that use inserts or anchors, since it gives continuity to the steel beam and, by crossing the section as shown in Figure 4.a, it takes the form of a support plate. This has the advantage that it distributes the applied point load better than the typical hook-shaped anchors of Figure 4b, verified by the average value of the experimental tests which is higher than the MC models over the MD models in (Table 1).

Failure due to horizontal load on the beam can be ruled out, as tests showed that they do not dominate the design. The lateral loads on hybrid nodes in beams of computer models of buildings with hybrid nodes (Castañeda and Mielles, 2017) are much lower than those obtained during the experimental test.

The STM gives greater longitudinal steel area in the beam, over 15% than the bending theory formulas because it recognizes the D region with the P load applied to the sides of the beam. This reduces the height of the struts and ties and complies with the ACI recommendation for beams with such loads. The STM has generalized formulas for a beam of any span with a single hybrid node, but based on that STM it can be extended for beams with more than one node.

5. Referencias

- ACI-318S-14. (2014)**, Requisitos de Reglamento para Concreto Estructural. Farmington Hills: American Concrete Institute.
- ACI-445. (2002)**, Diseño de Hormigón Estructural usando Modelos de Bielas y Tirantes. Farmington Hills.
- Aguiar, R. (2014)**, *Análisis Matricial de Estructuras* p. 6-8, Quito - Ecuador: Universidad de las Fuerzas Armadas-ESPE.
- Aguiar, R., Revelo, M., & Tapia, W. (2010)**, Análisis de conexiones viga-columna de acuerdo al código ACI Paper presented at the Jornadas de investigación, Quito.
- ASCE. (1994)**, Guidelines for desing of joints between steel beams an reinforced concrete columns. *Journal of structural engineering*, 120 No. 8. doi: [https://doi.org/10.1061/\(ASCE\)0733-9445\(1994\)120:8\(2330\)](https://doi.org/10.1061/(ASCE)0733-9445(1994)120:8(2330))
- Aznar, A., García, H., Ignacio, J., Herrera, J. O., & Cervera, J. (2008)**, Conexión de forjados de hormigón a soportes metálicos. Paper presented at the IV CONGRESO ACHE. Congreso Internacional de Estructuras, Valencia.
- Castañeda, E., & Mieles, Y. (2016)**, Reflexiones sobre daños observados en edificios de vigas con nudos híbridos y losas "steel deck" ante el sismo del 16 de abril de 2016. Paper presented at the Proceedings of the "First Annual State-of-the-Art in Civil Engineering Structures and Materials", Quito.
- Castañeda, E., & Mieles, Y. (2017)**, Una mirada al comportamiento estructural de columnas, vigas, entresijos y edificaciones durante el sismo de Ecuador 2016. *Revista Ingeniería de la Construcción*, Vol. 32 No. 3 doi: <http://dx.doi.org/10.4067/S0718-50732017000300157>.
- Chen, Q., Cai, J., Bradford, M. A., Liu, X., & Wu, Y. (2015)**, Axial Compressive Behavior of Through-Beam Connections between Concrete-Filled Steel Tubular Columns and Reinforced Concrete Beams. *Journal of structural engineering*, 141(10), 04015016. doi: [https://doi.org/10.1061/\(ASCE\)ST.1943-541X.0001249](https://doi.org/10.1061/(ASCE)ST.1943-541X.0001249)
- EHE-08. (2008)**, Instrucción de Hormigón Estructural. Madrid.
- FIP. (1999)**, Practical design of structural concrete. *FIP Commission 3, Practical Design*.
- Garzón, J. (2013)**, *Estudio del comportamiento a flexocompresión de soportes de hormigón armado reforzados con angulares y presillas metálicos*. (Tesis Doctoral), Valencia, Universidad Politécnica de Valencia.
- Kuramoto, H., & Nishiyama, I. (2004)**, Seismic performance and stress transferring mechanism of through-column-type joints for composite reinforced concrete and steel frames. *Journal of structural engineering*, 130(2), 352-360. doi: [https://doi.org/10.1061/\(ASCE\)0733-9445\(2004\)130:2\(352\)](https://doi.org/10.1061/(ASCE)0733-9445(2004)130:2(352))
- Li, W., Li, Q.-n., Jiang, W.-s., & Jiang, L. (2011)**, Seismic performance of composite reinforced concrete and steel moment frame structures—state-of-the-art. *Composites Part B: Engineering*, 42(2), 190-206. doi: <https://doi.org/10.1016/j.compositesb.2010.10.008>
- MacGregor, J. (2002)**, Derivación de modelos de bielas y tirantes para el Código ACI 2002. *ACI Structural Journal*.
- Mander, J. B., Priestley, M. J., & Park, R. (1988)**, Theoretical stress-strain model for confined concrete. *Journal of structural engineering*, 114(8), 1804-1826. doi: [https://doi.org/10.1061/\(ASCE\)0733-9445\(1988\)114:8\(1804\)](https://doi.org/10.1061/(ASCE)0733-9445(1988)114:8(1804))
- Marcus, J., & Thiers, R. (2015)**, Control del daño sísmico estructural en pórticos prefabricados de hormigón armado a través de uniones híbridas autocentranes. *Obras y Proyectos*(18), 46-55. doi: <https://doi.org/10.4067/S0718-28132015000200004>
- Mieles, Y., & Castañeda, E. (2016a)**, Estudio de alteraciones en el comportamiento estructural de vigas de hormigón armado con nudos híbridos mediante el empleo de gráficos momento-curvatura. *Revista Internacional de Ingeniería de Estructuras*, 21,1, 45-59.
- Mieles, Y., & Castañeda, E. (2016b)**, Reflexiones sobre daños observados en edificios de vigas con nudos híbridos y losas "steel deck" ante el sismo del 16 de abril de 2016. Paper presented at the Proceedings of the "First Annual State-of-the-Art in Civil Engineering Structures and Materials", Quito.
- Nie, J., Bai, Y., & Cai, C. (2008)**, New connection system for confined concrete columns and beams. I: Experimental study. *Journal of structural engineering*, 134(12), 1787-1799. doi: [https://doi.org/10.1061/\(ASCE\)0733-9445\(2008\)134:12\(1787\)](https://doi.org/10.1061/(ASCE)0733-9445(2008)134:12(1787))
- Nilson, A., Darwin, D., & Dolan, C. (2010)**, *Design of Concrete Structures*, p. 332-356 (McGraw-Hill Ed. Fourteenth ed.).
- Novak, L. C. (2010)**, SP-273: Further Examples for the Design of Structural Concrete with Strut-and-Tie Models. *Special Publication*, 273.
- NSR (2012)**, Norma Sismo Resistente de Colombia, Título C Concreto Estructural.
- Rasoul, S., & Bakhshayesh, N. (2013)**, Analytical investigation of a new Through-Column-Type Joint for composite reinforced concrete and steel frames. Paper presented at the The 2013 World Congress on Advances in Structural Engineering and Mechanics, Jeju-Korea.
- Rasoul, S., Bakhshayesh, N., & Mehdi, M. (2016)**, Moment-connection between continuous steel beams and reinforced concrete column under cyclic loading. *Journal of Constructional Steel Research*, 118, 105-119. doi: <https://doi.org/10.1016/j.jcsr.2015.11.002>
- Reineck, K. (2002)**, Ejemplos para el Diseño de Hormigón Estructural usando Modelos de Bielas y Tirantes. *ACI Structural Journal*.
- Schlaich, J., Schäfer, K., & Jennewein, M. (1987)**, Toward a consistent design of structural concrete. *PCI journal*, 32(3), 74-150. doi: <https://doi.org/10.15554/pci.05011987.74.150>
- Soto, J. (2012)**, *Proyecto de conexiones de vigas de acero a muros de concreto en estructuras mixtas*. Universidad Católica Andrés Bello.
- Ugel, R. (2015)**, Vulnerabilidad sísmica en edificaciones porticadas compuestas de acero y hormigón armado. (Doctor), UNIVERSITAT POLITÈCNICA DE CATALUNYA Barcelona.
- Wight, J., & MacGregor, J. (2012)**, *REINFORCED CONCRETE Mechanics and Design* (P. Education Ed. Sixth ed.).

